Effect of lateral connections on the accuracy of the population code for a network of spiking neurons

Mona Spiridon and Wulfram Gerstner

Center for Neuromimetic Systems,
Swiss Federal Institute of Technology, Lausanne,
EPFL-DI
CH-1015 Lausanne EPFL, Switzerland

Abstract

We study how neuronal connections in a population of spiking neurons affect the accuracy of stimulus estimation. Neurons in our model code for a one-dimensional orientation variable ϕ. Connectivity between two neurons depends on the absolute difference $|\phi - \phi'|$ between the preferred orientation of the two neurons. We derive an analytical expression of the activity profile for a population of neurons described by the spike response model with noisy threshold. We estimate the stimulus orientation and the trial-to-trial fluctuations using the population vector method. For stationary stimuli, uniform inhibitory connections produce a more reliable estimation of the stimulus than short-range excitatory connections with long-range inhibitions, although the latter interaction type produces a sharper tuning curve. These results are consistent with previous analytical studies of the Fisher information.

1 Introduction

The response of most neurons in the central nervous system shows a high degree of variability (Werner & Mountcastle 1965; Schiller et al. 1976; Vogels et al. 1989; Britten et al. 1993; O'Keefe et al. 1997). Since neuronal noise has a detrimental impact on information processing, redundancy is needed to average out the noise. The primary visual cortex, for example, is organised in columns composed of neurons that respond preferentially to the same stimulus orientation (Hubel & Wiesel 1968, 1974). Using a population of neurons with similar properties to encode information has the advantage of reducing the noise. On the other hand, if neurons in the population are connected to each other or share input, they cannot be treated as independent. Because it is likely that nearby neurons share more common inputs than distant neurons, correlated variability is expected to decreases with interneuronal distance (Braitenberg & Schuz 1991; Zohary et al. 1994; Douglas et al. 1995). Although the experimentally-measured correlation coefficients are quite small, correlated variability is thought to limit the information processing capacity of neuronal ensembles (Zohary et al. 1994). However, several researchers have shown that the effect of correlated noise is not always harmful to information processing (Snippe & Koenderink 1992; Abbott & Dayan 1999; Yoon

& Sompolinsky 1998). Snippe & Koenderink (1992) have indicated that, if the spatial range of correlated noise is larger than the receptive field width of neurons, it can lead to improvement of the discrimination thresholds in psychophysical tasks. Recently, Abbott & Dayan (1999) and Yoon & Sompolinsky (1998) have used Fisher information to provide an estimation of the accuracy of the population code using neurons described by a rate model. Under the hypothesis that the neuronal activity follows a multivariate Gaussian distribution, they have shown some effects of the shape of the correlation matrix on the the population code accuracy. For instance, Yoon & Sompolinsky (1998) have found that negative correlations enhance the Fisher information relative to the uncorrelated case, whereas positive correlations almost always decrease it. Only in the extreme case of very long correlations can positive correlations produce a higher information value than in the case of an uncorrelated population. Thus, depending on the form of the correlation matrix, correlated variability can either increase or decrease the information capacity in comparison to the uncorrelated case.

In these studies correlated noise was introduced explicitly into the model by the definition of a correlation matrix (Snippe & Koenderink 1992; Abbott & Dayan 1999; Yoon & Sompolinsky 1998). Nevertheless, these correlations must somehow be generated inside the neural network. Correlations induced by common input have been considered in other studies (Shadlen & Newsome 1998). In this paper, we explore the possibility that correlated noise originates from the *lateral* connections inside the neural network. We study how correlations induced by lateral connections affect the accuracy of the population code. We compare two types of interactions: Uniform inhibition (homogeneous interactions) and short-range excitation with long-range inhibition (modulated interactions). It has been suggested that these interaction types play an important role in the mechanisms for orientation selectivity in the primary visual cortex. Indeed, V1 neurons receive a broad input from the LGN but their tuning curve is much sharper. Several models have been proposed to explain the sharpening of the tuning curve in V1. Some models suggest that orientation selectivity is mainly caused by lateral inhibition (Ferster & Koch 1987; Wörgötter & Koch 1991; Wehmeier et al. 1998) whereas other authors have proposed that orientation tuning is the result of short-range excitations together with longer range inhibitions (Ben-Yishai et al. 1995; Somers et al. 1995), producing a Mexican hat-shaped interaction between orientation columns.

As in previous studies of Ben-Yishai et al. (1995) and Hansel & Sompolinsky (1998), we use a one-dimensional population of spiking neurons, where each neuron codes for a particular orientation of the stimulus. In Section 2, the model is defined. In Section 3, an analytical expression of the activity profile is derived. In Section 4, we define how we assess the accuracy of the estimation and discuss how lateral interactions induce correlation.

2 The Model

2.1 The Network Model

We consider a population of N interconnected neurons evenly distributed on a one-dimensional line. Each neuron i codes for a particular scalar feature ϕ_i. The feature ϕ can represent any external physical variable with which neural activity is correlated. For simplicity we will assume periodic boundary conditions, and interpret ϕ as the

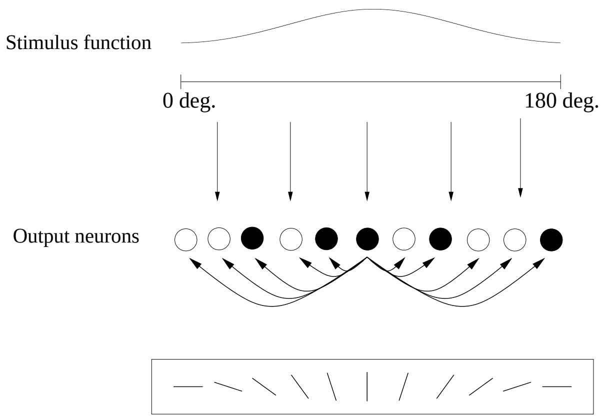

Figure 1: Sketch of the network architecture. The input stimulus potential (Eq. (2)) is broad and periodic (top). The neuronal network is fully-connected. Here, we have represented only the lateral connections from one neuron (middle). The connection strengths are described by Eq. (6). Neurons are characterised by their preferred orientation (bottom)

orientation of a stimulating light bar. All functions of ϕ are periodic functions with period π.

Each neuron i is selective for a range of orientations and responds maximally when a particular value ϕ_i of the stimulus orientation, called the preferred orientation, is present. The values of preferred orientations ϕ_i are uniformly distributed among the neurons in the interval $0 < \phi_i \leq \pi$. The total input h_i to each neuron consists of two parts, i.e. an external input $h_i^{\rm ext}$ (stimulus) and the input $h_i^{\rm int}$ from the other neurons of the network (Figure 1).

$$h_i(t) = h_i^{\rm int}(t) + h_i^{\rm ext}(t) \tag{1}$$

If the stimulus has orientation ϕ_0, the external input to neuron i is represented by a Von Mises function (Fisher 1993):

$$h_i^{\rm ext}(\phi_0) = \frac{h^{\rm max}}{\exp(\alpha^{-1} - 1)} \exp\left[\alpha^{-1} \cos\left(2(\phi_0 - \phi_i)\right) - 1\right] \tag{2}$$

This function is similar to a Gaussian but is π-periodic. The parameter α corresponds to the width of the function. We choose a large value of α so that the stimulus is broadly tuned. The first term of Eq. (2) normalises the function, so that the maximum amplitude is equal to $h^{\rm max}$. A neuron i responds maximally when the orientation of the input stimulus ϕ_0 is equal to its preferred orientation ϕ_i.

The lateral input $h_i^{\rm int}$ is characterised by the coupling strength J_{ij} and the time course $\varepsilon_{ij}(t)$ of the postsynaptic potential

$$h_i^{\rm int}(t) = \frac{1}{N} \sum_{j=1}^{N} \sum_{t_j^{(f)}} J_{ij}\, \varepsilon(t - t_j^{(f)}) \tag{3}$$

where the sum runs over all firing times $t_j^{(f)}$ and over all neurons in the network. Note that we have taken the interaction strength to scale inversely with the total number of neurons N. The kernel ε can be chosen arbitrarily. Here, we take:

$$\varepsilon(s) = \frac{1}{\tau_s - \tau_m}\left[\exp\left(-\frac{s}{\tau_s}\right) - \exp\left(-\frac{s}{\tau_m}\right)\right]\mathcal{H}(s) \tag{4}$$

where τ_s and τ_m are respectively the synaptic and membrane time constant. To ensure causality we have added the Heaviside function $\mathcal{H}(\cdot)$ with $\mathcal{H}(s) = 1$ for $s > 0$ and 0 otherwise. ε is normalised so that $\int_0^\infty \varepsilon(s)ds = 1$. For $\tau_m = \tau_s = \tau$, Eq. (4) reduces to:

$$\varepsilon(s) = \frac{s}{\tau^2}\exp\left(-\frac{s}{\tau}\right)\mathcal{H}(s) \tag{5}$$

For the sake of simplicity, we assume that neurons can have both excitatory and inhibitory connections with each others. This coupling model is of course not biologically plausible. However, Ben-Yishai et al. (1995) and Hansel & Sompolinsky (1998) have shown that many qualitative properties of the stationary states remain when the one-type population is replaced by a population with excitatory and inhibitory neurons. The interaction strength J_{ij} is assumed to be strongest in magnitude for neurons with similar preferred orientations. This hypothesis is consistent with the anatomical and physiological evidence available in the primary visual cortex (Ferster 1986; Martin 1988). In order to describe the orientation dependence of the coupling strength, we choose the type of interaction used by (Ben-Yishai et al. 1995) to study the properties of the orientation tuning curves in the visual cortex. It is expressed using the first two terms of the Fourier series:

$$J_{ij} = J(\phi_i - \phi_j) = J_0 + J_2\,\cos(2(\phi_i - \phi_j)) \tag{6}$$

Only even terms are non-null, as the period of J is π. The coupling equation is represented in Figure 2 for two different values of J_2.

2.2 The Neuronal Model

The membrane potential u_i of neuron i describes the state of the neuron. In the spike response model, the membrane potential is given by (Gerstner 1995):

$$u_i(t) = \eta(t - \hat{t}_i) + h_i(t) \tag{7}$$

where $h_i(t)$ is the total input (Eq. 1) described in Section 2.1 and $\hat{t}_i$ is the firing time of the last spike of neuron i. The function η describes the refractory period following a spike. We use:

$$\eta(s) = -\eta_0\,\exp\left(-\frac{s - \delta_{\text{abs}}}{\tau_m}\right)\mathcal{H}(s - \delta_{\text{abs}}) + K\,\mathcal{H}(\delta_{\text{abs}} - s)\,\mathcal{H}(s) \tag{8}$$

where δ_{abs} is the absolute refractory period, K is a large negative constant and τ_m is the membrane time constant. We set $\eta_0 = 1$.

In order to reproduce the variability in the firings of cortical neurons, we add noise to the neuronal model. To do so, we introduce an escape rate ρ that depends on the difference between the present value of the membrane potential $u(t)$ and the threshold ϑ.

$$\rho_{h_i}(t|\hat{t}_i) = f[u(t) - \vartheta] = f[\eta(t - \hat{t}_i) + h_i(t) - \vartheta]. \tag{9}$$

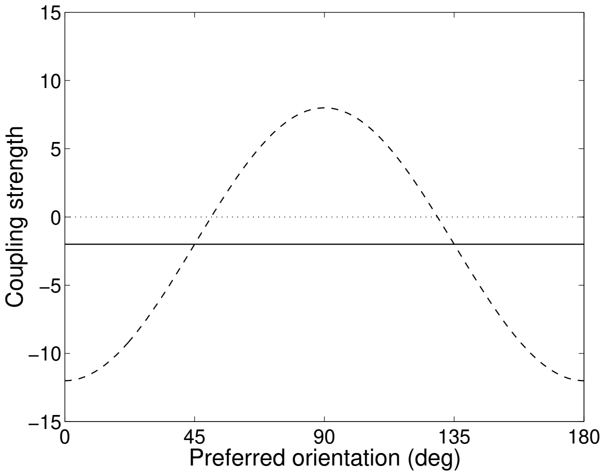

Figure 2: Coupling strength function for a neuron at 90° preferred orientation as a function of the preferred orientation. Two types of interaction described by Eq. (6) are plotted here. The solid line represents uniform inhibition ($J_0 = -2$, $J_2 = 0$) and the dashed line shows modulated interactions ($J_0 = -2$, $J_2 = 10$).

The second equality follows from (7). The escape rate ρ is implicitly time-dependent, since the membrane potential $u(t)$ varies over time. The choice of the function f is arbitrary; since the results that we have obtained are qualitatively independent of the form of the escape rate, we use for simplicity a piecewise linear function

$$\rho = \gamma_0 \cdot (u - \vartheta)\mathcal{H}(u - \vartheta) \tag{10}$$

where γ_0 is a parameter that determines the noise level. The higher the value of γ_0 the lower the noise. It should be noted that with an appropriate choice of f, the escape rate ρ can reproduce, to a high degree of accuracy, noise due to stochastic spike arrival (Plesser & Gerstner 2000).

Given the escape rate function, we can calculate the survivor function, that is the probability that the neuron, after having emitted a spike at $\hat{t}_i$, will not emit a spike up to time t (Cox 1962; Gerstner & Van Hemmen 1992; Gerstner 2000).

$$S_{h_i}(t|\hat{t}_i) = \exp\left[-\int_{\hat{t}_i}^{t} \rho_{h_i}(s|\hat{t}_i)ds\right] \tag{11}$$

The survivor function obviously depends on $\hat{t}_i$, the last firing time of neuron i. The lower index h_i in the survivor function is intended to remind the reader that $S_{h_i}(t|\hat{t}_i)$ also depends on the input potential $h_i(t)$.

3 Activity Profile

The activity profile describes the firing rate of the neurons as a function of their preferred orientations. Since the network is completely axisymmetric, the coupling between two neurons only depends on the absolute difference $|\phi - \phi'|$ between their preferred orientation. Therefore, the form of the activity profile is identical to the form of the tuning curve of a single neuron. For a time-stationary state the activity profile can be obtained from a set of self-consistent equations. Indeed, in a stationary state, we can define the average input potential h_i^c as:

$$h_i^c \equiv < h_i^{\text{int}}(t) > + h_i^{\text{ext}} \tag{12}$$

where h_i^{ext} is the constant external stimulus and $< x(t) >$ is the average of $x(t)$ over time. By rewriting Eq. (3) in a different form, we have

$$< h_i^{\text{int}}(t) > = \frac{1}{N} \sum_{j=1}^{N} J_{ij} \sum_{t_j^{(f)}} \int_0^{\infty} \varepsilon(s) < \delta(t - t_j^{(f)} - s) > ds \tag{13}$$

The quantity $\sum_{t_j^{(f)}} < \delta(t - t_j^{(f)} - s) >$ corresponds to the mean firing rate r_j of neuron j. Thus, we have:

$$h_i = \frac{1}{N} \sum_{j=1}^{N} J_{ij}\, r_j + h_i^{\text{ext}} \tag{14}$$

where we have use the fact that $\int_0^{\infty} \varepsilon(s) ds = 1$. The mean firing rate r_i for neuron i can be calculated from the survivor function (Gerstner & Van Hemmen 1992)

$$r_i = \left[\int_0^{\infty} S_{h_i^c}(s) ds \right]^{-1}, \tag{15}$$

where for a constant potential $h_i(t) = h_i^c$, the survivor function $S_{h_i^c}(t|\hat{t}_i)$ depends on only on the time difference $t - \hat{t}_i$. So far, analytical expressions for the activity profile have been obtained with rate models (Ben-Yishai et al. 1995; Hansel & Sompolinsky 1998) and integrate-and-fire models in the absence of internal noise (Laing & Chow in press). Eq. (14) and (15) give a theoretical solution for the activity profile in a network of spiking neurons with internal noise. Figure 3 shows that the activity profile resulting from these equations matches to a high degree of accuracy the one obtained by simulating a population of spiking neurons described by the model in Section 2. The sharper tuning curve obtained with the local excitation with long-range inhibition can be understood as the result of the similarity between the shape of the tuning curve and that of the connection pattern: excitation is therfore maximum where the activity is large and inhibition is maximum where activity is low.

4 Accuracy of the stimulus estimator

An estimation of the stimulus orientation ϕ^{est} is obtained using the population vector method (Georgopoulos et al. 1983; Salinas & Abbott 1994). The accuracy of the estimator is measured by the variance of the trial-to-trial fluctuations. Because the variable ϕ is distributed on a circle, we use the circular standard deviation (CSD) to measure the fluctuations in the orientation (Mardia 1972)(see Appendix). The CSD of the orientation estimator is computed for different time window durations T, starting from the initiation of the stimulus. For stationary stimuli, the longer the duration of the time window, the better the estimation. For long time window duration (> 100 ms)

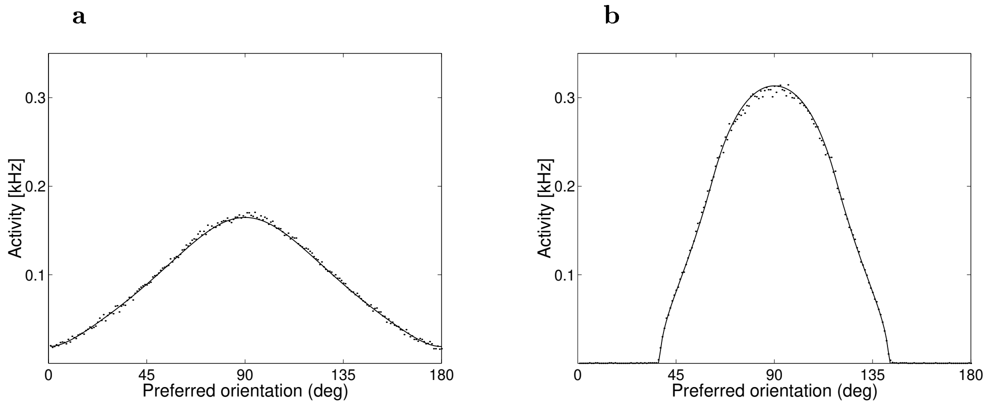

Figure 3: Activity profile obtained from simulations (dots) compared with theory (solid line). The rate in simulations is estimated from spike counts over 2 s following the onset of the stimulus with a population of 200 neurons. The amplitude of the external stimulus $h^{\max} = 2$,the width $\alpha = 4$ and the orientation is $\phi_0 = 90$ degree, cf. Eq (2). The values for the interaction strength are (**a**) $J_0 = -2$ and $J_2 = 0$ and (**b**) $J_0 = -2$ and $J_2 = 10$. Neurons have an absolute refractory period of 2 ms and the synaptic and membrane time constants are both equal to 4 ms. The neuronal noise is described by a linear escape rate model with $\gamma_0 = 1$.

the CSD decreases approximatively with $1/\sqrt{T}$. The stimulus is initiated at $t = 0$ ms. Before the start of the stimulus all neurons are silent[1].

4.1 Effect of lateral connections

We would like to understand how the lateral connections affect the accuracy of the population code. To do so we compare the CSD obtained using uniform inhibition (Eq. (6) with $J_2 = 0$) and the one obtained using modulated interactions (Eq. (6) with $J_2 > 0$). Figure 4a and b represent the theoretical activity profiles and the CSD obtained by these two interactions types. We find that although short range excitation sharpens the tuning curve (Figure 4a), the reliability of the estimation decreases (Figure 4b). Modulated interactions produce a less reliable estimation even when the activity profile generated by modulated interactions is exactly identical to the one obtained by uniform inhibition (Figure 4c and d). The spatial dependency of the interactions therefore appears to be important in the determination of the accuracy of the population code.

In order to better understand what determines the accuracy of the estimator, we compare the standard deviation obtained by the population vector method with the one obtained using Fisher information. The Fisher information, through the Cramer-Rao bound, gives a measure of the lowest variance of an unbiased estimator (Blahut 1988).

$$\sigma_\phi^2 \geq \frac{1}{I(\phi)} \tag{16}$$

[1] We do not take into account any spontaneous activity for $t < 0$, in order to simplify the comparison of the CSD for different parameters. Indeed, the spontaneous activity would change each time we change the value of a parameter

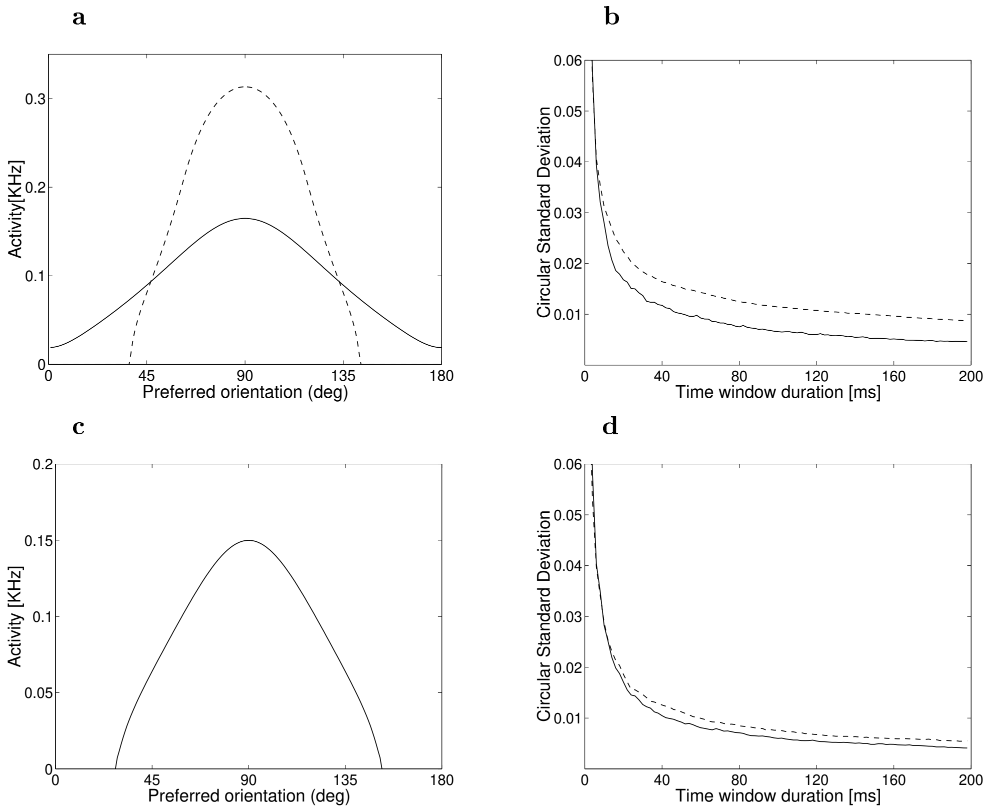

Figure 4: (**a**) Activity profile and (**b**) circular standard deviation (CSD) for a network with uniform inhibition ($J_0 = -2$, $J_2 = 0$) (solid line) and for a network with short-range excitation and long-range inhibition ($J_0 = -2$, $J_2 = 10$) (dashed line). In the two cases, the stimulus amplitude is equal to $h^{\max} = 2$. We see that even though the tuning curve is shaper for $J_2 = 10$, the estimation is worse. (**c**) Activity profile. The stimulus amplitude $h^{\max}$ has been adjusted in order to obtain the same activity profile for the two types of interaction. The activity profiles for uniform inhibition ($J_0 = -5, J_2 = 0, h^{\max} = 1.96$) and modulated interactions ($J_0 = 0, J_2 = 2, h^{\max} = 1.55$) lie on top of each other and are indistinguishable. (**d**) Circular standard deviation (CSD) for uniform interactions (solid line) and modulated interactions (dashed line). In all the cases the orientation of the stimulus is 90 degree and the CSD is calculated from 500 trials with a population of 200 neurons. The network and neuronal parameters are the same as in Figure 3.

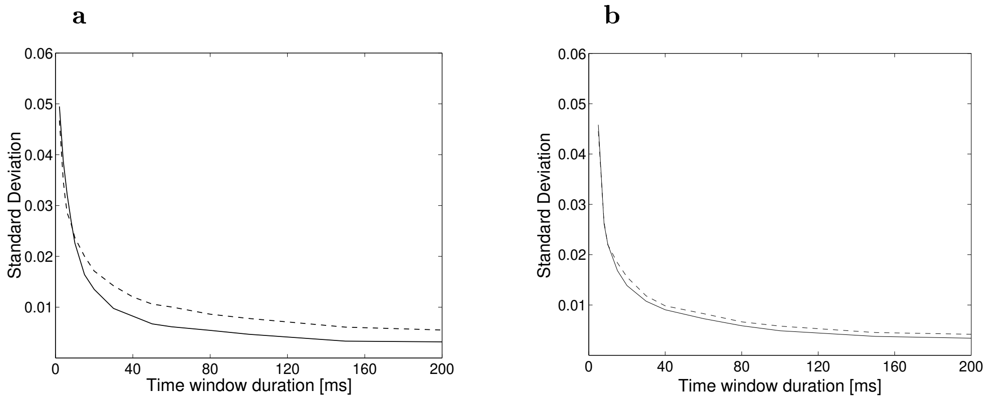

Figure 5: Lower bound of the standard deviation using Fisher information for a network with uniform inhibition (solid line) and for a network with short-range excitation and long-range inhibition (dashed line). The coupling parameters are the same as in Figure 4b for **a** and in Figure 4d for **b**. The covariance matrix has been estimated from a simulation over 500 trials.

where $I(\phi)$ is the Fisher information for orientation ϕ. If the neuronal activities follow a Gaussian distribution, the Fisher information can be expressed as a function of the covariance matrix and of the tuning curve derivative (Abbott & Dayan 1999; Yoon & Sompolinsky 1998).

$$I(\phi) = \sum_{i,j} f_i'(\phi) C_{ij}^{-1} f_j'(\phi) \tag{17}$$

where $f_i(\phi)$ represents the tuning function of neuron i and $f_i'(\phi) \equiv \frac{\partial f_i(\phi)}{\partial \phi}$. The covariance matrix $C_{ij}(\phi)$ of the firing rates (r_i, r_j) is defined as follows:

$$C_{ij}(\phi) = \frac{1}{K} \sum_{k=1}^{K} (r_i^k - f_i(\phi))(r_j^k - f_j(\phi)) \tag{18}$$

where r_i^k is the firing rate of neuron i on trial k and K is the total number of trials. We measure the covariance matrix (Eq. 18) from simulations over 100 ms (Figure 6) and calculate the Fisher information via Eq. (17). This gives a lower bound on the variance (cf. Eq. (16)). Due to the refractory period, the distribution in spike counts of our model is well approximated by a Gaussian distribution even for short time window durations. We found that the standard deviation calculated using Fisher information gives slightly lower values than the population vector method as it should be, since Fisher information gives the optimal estimator. However, we find that the effect of a network or neuronal parameter on the accuracy of the stimulus estimation is qualitatively similar for both methods (Figure 5). This means that the measure of the standard deviation is mostly independent of the decoding method.

The Fisher information allows an interpretation of our results. Eq. (17) shows that the accuracy of the population code is determined by (i) the derivative of the tuning curve and (ii) the correlation matrix. In case that the two tuning curves are the same as in Figure 4c, differences in Fisher information can only be generated by the second term, i.e. negative correlations induced by inhibitory interactions are advantageous to

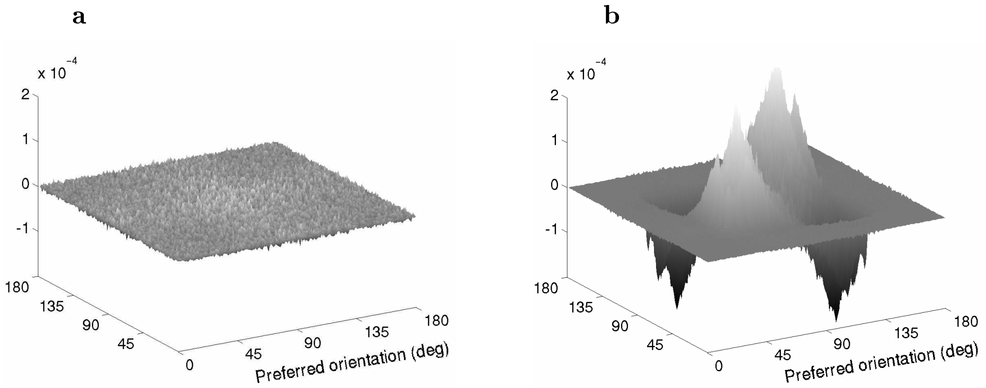

Figure 6: Covariance matrix of the firing rates for network of 200 neurons with uniform inhibition ($J_0 = -2, J_2 = 0$) (**a**) and modulated interactions ($J_0 = -2, J_2 = 10$) (**b**). A stimulus is applied with $\alpha = 4$, $h^{\max} = 2$ and $\phi_0 = 90°$. The values on the diagonal have been removed for the purpose of visualisation. The covariance matrix is estimated from a simulation over 100 ms.

the accuracy of the population code. Figure 5b confirms that correlations induced by uniform inhibition lead to a lower value of the Fisher information than those induced by modulated interactions.

Figure 6 represents the covariance matrix for the two type of interactions (uniform inhibition and by modulated interactions). The diagonal terms have been removed for the purpose of visualisation. For uniform inhibitory interactions, the non-diagonal terms of the covariance matrix are uniformly negative but of very low amplitude[2], even for very strong inhibition (Figure 6a) Spiridon (2000). On the other hand, correlated noise produced by modulated interactions is positive for nearby neurons and negative between two distant neurons. Moreover, the same pair of neurons can have different correlations, depending on the type of stimulus. This can be seen in Figure 6b. Due to the complete symmetry of the system, measuring correlation between a given pair of neurons while changing the stimulus orientation would correspond to measuring correlations for different pairs of neurons (separated by the same preferred orientation difference) for a given stimulus orientation. Compare for example in Figure 6b the pair of neurons at 45° and 50° and the pair at 90° and 95°. Even though lateral interactions are the same, correlations are quite different. The effect of a correlation matrix as generated by this type of interactions on the Fisher information has not been studied yet analytically. Yoon & Sompolinsky (1998) have shown that local positively correlated noise decreases the estimation reliability. In our case, the estimation reliability is not only decreased by locally positively correlated noise but also by the negatively correlated noise between neurons with dissimilar preferred orientation. Indeed, we have estimated that the accuracy is improved by about 20 percent when the negative correlated noise between distant neurons is removed and only the local positive correlations are retained.

[2]Mathematically, a covariance matrix cannot have only large negative values, because it must be positive-definite. This explains why, even with strong uniform negative couplings, the amplitude of the negative correlations remains quite small.

5 Discussion

In contrast to previous work (Ferster & Koch 1987; Ben-Yishai et al. 1995; Somers et al. 1995), we were not interested in the shape of the tuning curve, but rather in correlations. In particular, we did not optimise parameters so as to obtain realistic profiles and we did not discuss how the form of the tuning curve changes with stimulation. Instead, we have studied how the accuracy of a population code depends on the lateral connection of a one-dimensional population of spiking neurons with periodic coupling. We have derived an analytical expression of the activity profile for stationary stimuli in a network of spiking neurons with internal noise. We have also studied the circular standard deviation (CSD) of the stimulus orientation, estimated from simulations using the population vector method. We have shown that sharp activity profiles do not necessarily yield a better estimation accuracy (Brunel & Nadal 1998; Pouget et al. 1999). By comparing the CSD between a network with uniform inhibition and a network with short-range excitation and long-range inhibition we have found that the latter interaction produces a less reliable stimulus estimation. Modulated interactions generate correlated noise that is positive for nearby neurons and negative for distant one and this type of correlated noise reduces the accuracy of the orientation estimate. We have also simulated networks without any lateral connections Spiridon (2000). The results are qualitatively similar to those obtained with uniform inhibition with a slightly lower value of the accuracy.

The effect of lateral connections on the stimulus estimation reliability can also be understood with intuitive arguments: A neuron k with a preferred orientation different from the stimulus orientation may increase its activity as a result of its intrinsic noise. For modulated interaction, this will also increase the activity of its neighbouring neurons because of the local excitatory inputs. On the other hand, the activity of distant neurons will decrease because of the long range inhibition. Thus, the total effect is that the instantaneous activity profile will slightly shift towards the preferred orientation of neuron k neuron. In contrast, with uniform inhibition, the spontaneous increase in the activity of a given neuron will not develop further, as neurons close to the orientation of the stimulus will send it a strong inhibitory signal. This simple reasoning shows that statistical fluctuations are amplified by a network with short-range excitatory connections, and suppressed by a network with uniform inhibitory connections.

Our studies show that uniform inhibition is more advantageous than modulated interactions, if stimuli are to be represented as accurately as possible. Stimulus representation is, of course, only one among many possible tasks of the nervous system. For a working memory task, for example, modulated interactions with local excitation are useful to stabilise activity patterns that have been triggered by an external stimulus (Redish et al. 1996; Camperi & Wang 1998).

Appendix

The performance of the population vector in estimating the orientation is measured by the variance of the trial-to-trial fluctuations. Special treatment is required to describe the variability of a directional measure such as the stimulus angle. Because the variable ϕ is distributed on a circle, we use the circular standard deviation (CSD) to measure the fluctuations in the orientation.

Suppose we have a set of angles ϕ_k, $k = 1 \,..\, K$ in a range of $[0\,;\pi]$. We calculate:

$$C = \sum_{k=1}^{K} \cos\, 2\phi_k, \quad S = \sum_{k=1}^{K} \sin\, 2\phi_k, \quad R^2 = C^2 + S^2. \tag{19}$$

The measure of the circular variance is given by

$$V = 1 - [1 - (1 - R/K)]^{1/4} \tag{20}$$

The circular standard deviation is defined as

$$CSD = [-2\, \log(1 - V)]^{1/2} \tag{21}$$

where log is the natural logarithm. If the variance is small, Eq. (21) reduces to

$$CSD = (2V)^{1/2} \tag{22}$$

A theoretical justification of these results is given in (Mardia 1972). The CSD as defined in Eq. (21) is used to assess the reliability of the angle estimation.

References

Abbott L.F. & Dayan P. (1999), The effect of correlated variability on the accuracy of a population code, *Neural Computation 11:1*, 91-101

Ben-Yishai R., Bar-Or R.L. & Sompolinsky H. (1995), Theory of orientation tuning in visual cortex, *Proceedings of the National Academy of Science USA 92*, 3844-3848

Blahut R.E. (1988), *Principles and Practice of Information Theory*, Addison-Wesley, Cambridge, MA

Braitenberg V. & Schuz A. (1991), *Anatomy of the cortex: statistics and geometry*, Springer, Berlin

Britten K.H., Shadlen M., Newsome W.T. & Movshon J.A. (1993), Response of neurons in macaque MT to stochastic motion signals, *Visual Neuroscience 10*, 1157-1169

Brunel N. & Nadal J.P. (1998), Mutual information, Fisher information and population coding, *Neural Computation 10*, 1731-1757

Camperi M. & Wang X.J. (1998), A model of visuospatial working memory in prefrontal cortex: recurrent network and cellular bistability, *Journal of Computational Neurocience 5*, 383-405

Cox D.R. (1962), *Renewal theory*, Mathuen, London

Douglas R.J., Koch C., Mahowald M., Martin K.A.C. & Suarez H.H. (1995), Recurrent excitation in neocortical circuits, *Science 269*, 981-985

Ferster D. (1986), Orientation selectivity of synaptic potentials in neurons of cat primary visual cortex, *Journal of Neuroscience 6*, 1284-1301

Ferster D. & Koch C. (1987), Neuronal connections underlying orientation selectivity in cat visual cortex, *Trends in Neurosciences 10*, 487-492

Fisher N. (1993), *Statistical analysis of circular data*, Cambridge University Press, Cambridge

Georgopoulos A.P., Caminit R., Kalaska J. & Massey J. (1983), Spatial coding of movements: A hypothesis concerning the coding movement direction by motor cortical populations, *Experimental Brain Research 7*, 327-336

Gerstner W. (1995), Time structure of the activity in neural network models, *Physical Review E 51(1)*, 738-758

Gerstner W. (2000), Population dynamics of spiking neurons: fast transients, asynchronous states, and locking., *Neural Computation 12*, 43-89

Gerstner W. & Van Hemmen J. (1992), Associative memory in a network of spiking neurons, *Network 3*, 139-164

Hansel D. & Sompolinsky H., Modeling feature selectivity in local cortical circuits, . In: Koch C. & Segev I. (eds), Methods in neuronal modeling, chap. 13, MIT Press, Cambridge, MA and London, GB (, 1998)

Hubel D.H. & Wiesel T.N. (1968), Receptive fields and functional architecture of monkey striate cortex., *Journal of Physiology (London) 195(1)*, 215-243

Hubel D.H. & Wiesel T.N. (1974), Sequence regularity and geometry of orientation columns in the monkey striate cortex, *Journal of Comparative Neurology 158(3)*, 267-293

Laing C.R. & Chow C.C. (in press), Stationary bumps in networks of spiking neurons, *Neural Computation*

Mardia K. (1972), *Statistics of Directional Data*, Academic Press, London and New York

Martin K. (1988), From single cells to simple circuits in the cerebral cortex, *Quarterly Journal of Experimental Physiology 73*, 637-702

O'Keefe J., Bair W. & Movshon J.A. (1997), Response variability of MT neurons in macaque monkey, *Society for Neuroscience Abstracts 23*, 1125

Plesser H.E. & Gerstner W. (2000), Noise in integrate-and-fire neurons: from stochastic input to escape rates, *Neural Computation 12*, 367-384

Pouget A., Deneve S., Ducom J.C. & Latham P. (1999), Narrow vs wide tuning curves: what's best for a population code, *Neural Computation 11*, 85-90

Redish A., Elga A. & Touretzky D. (1996), A coupled attractor model of the rodent head direction system, *Network 7(4)*, 671-685

Salinas E. & Abbott L. (1994), Vector Reconstruction from Firing Rates, *Journal of Computational Neuroscience 1*, 89-107

Schiller P.H., Finlay B.L. & Volman S.F. (1976), Short-term response variability of monkey striate neurons, *Brain research 105*, 347-349

Shadlen M. & Newsome W.T. (1998), The variable discharge of cortical neurons: implications for connectivity, computation, and information coding, *Journal of Neuroscience 18*, 3870-3896

Snippe H.P. & Koenderink J.J. (1992), Information in channel-coded systems: correlated receivers, *Biological Cybernetics 67*, 183-190

Somers D.C., Nelson S.B. & Sur M. (1995), An Emergent Model of Orientation Selectivity in Cat Visual Cortical Simple Cells, *Journal of Neuroscience 15*, 5448-5465

Spiridon M. (, 2000), Ph.D. thesis, Swiss Federal Institute of Technology Lausanne

Vogels R., Spileers W. & Orban G.A. (1989), The response variability of striate cortical neurons in the behaving monkey, *Experimental Brain Research 77*, 432-436

Wehmeier U., Dong D., Koch C. & Essen D.V., Modeling the mammalian visual system, . In: Koch C. & Segev I. (eds), Methods in neuronal modeling, pp. 335–359, MIT Press, Cambridge (, 1998)

Werner G. & Mountcastle V.B. (1965), The variability of central neural activity in a sensory system and its implications for the central reflection of sensory events, *Journal of Neurophysiology 26*, 958-977

Wörgötter F. & Koch C. (1991), A detailed model of the primary visual pathway in the cat: comparison of afferent excitatory and intracortical inhibitory connection schemes for orientation selectivity, *Journal of Neuroscience 11*, 1959-1979

Yoon H. & Sompolinsky H. (1998)The effect of correlations on the fisher information of population codes. In: Jordan M.I., Kearns M.J., & Solla S.A. (eds), Advances in Neural Information Processing Systems 11, 167-173, Cambridge MIT Press

Zohary E., Shadlen M. & Newsome W. (1994), Correlated neuronal discharge rate and its implications for psychophysical performance, *Nature 370:6485*, 140-143